Journal of Oil Palm Research
DOI: https://doi.org/10.21894/jopr.2022.0035

TRANSPIRATION OF OIL PALM (*Elaeis guineensis* Jacq.) BASED ON SAP FLOW MEASUREMENT: THE RELATION TO SOIL AND CLIMATE VARIABLES

IPUT PRADIKO[1]*; SUROSO RAHUTOMO[1]; RANA FARRASATI[1]; EKO NOVIANDI GINTING[1]; FANDI HIDAYAT[1] and MUHDAN SYAROVY[1]

ABSTRACT

This study measured sap flow (SF) using Heat Ratio Method (HRM) to estimate the transpiration of two 14 years old oil palms for 29 days. Plant water potential (Ψ_{frond}) was also observed with a psychrometer. Environmental factors such as solar radiation (Qs), vapour pressure deficit (VPD), rainfall (RF), and soil moisture (SM) were also gauged to quantify their contribution to oil palm water flux. Results showed that SF increased after sunrise, peaked after midday, reached a maximum of 386.77-457.79 cm^3 hr^{-1}, and declined thereafter. Environmental factors and Ψ_{frond} explained 76.59%-80.02% variation in quarter-hourly sap flux. The contribution of environment variables on SF followed the order of Qs > VPD > SM > RF. The Ψ_{frond} was opposite with SF and at the lowest point after SF reached the peak for 30-45 min. Minimum values of Ψ_{frond} on palms No. 1 and 2 were -0.84 and -0.78 MPa, respectively. The contribution of environment variables on Ψ_{frond} was less than 24%, with the highest coming from Qs and VPD. Daily stand transpiration of oil palm was at 0.82-1.66 mm day^{-1} which comprised about 30% of stand evapotranspiration. Hence, Qs and VPD showed a significant role in affecting oil palm transpiration in this study.

Keywords: oil palm, plant water potential, sap flow, transpiration, water requirement.

Received: 23 December 2021; **Accepted:** 10 May 2022; **Published online:** 29 June 2022.

INTRODUCTION

Water is the basic requirement for crop growth and development. Water promotes seed germination, mediates nutrition uptake from the soil, circulates minerals and organic nutrients throughout the plant, controls turgor pressure, generates plant cell expansion, supports plant form and function, and controls stomatal movements (Blatt *et al.*, 2014). Hence, adequate water is needed to support plant development and maximise the crop's yield (Nascimento *et al*, 2018).

Amounts of water required by a specific crop vary from one site to another due to the crop growth stages, environmental conditions, and agricultural practices (Pereira and Alves, 2005). There are various methods to estimate crop water requirements, *i.e.*, evapotranspiration based-methods (Doorenbos and Pruitt, 1977), lysimeter method (Ruiz-Penalver *et al.*, 2015), and transpiration based-methods. The transpiration based-methods consist of the Penman-Monteith combination equation (Milne *et al.*, 1985), energy balance method (Milne *et al.*, 1985), water potential based-method (Garnier *et al.*, 1988), gravimetric (Ferrara and Flore, 2003), allometric based-method (Legros *et al.*, 2009) and gas exchange measurements (Ferrara and Flore, 2003; Suresh *et al.*, 2012a). Bayona-Rodríguez and Romero (2016) stated that all methods generally provided information

[1] Indonesian Oil Palm Research Institute (IOPRI), Brigjen Katamso No. 51, 20158, North Sumatra, Indonesia.

* *Corresponding author e-mail: iputpradiko@gmail.com*

about the actual water demand of a specific crop under partially controlled conditions. Thus, direct measurement is needed to determine water use under field conditions.

Not all of the methods stated can be used to estimate water use on perennial crops under field conditions, particularly for oil palm. Unfortunately, measurement of actual water requirements on oil palm is not easy due to the unique vegetative structures, long duration of generative stages (almost three years) (Carr, 2011), monocot vascular tissue (Madurapperuma *et al*., 2009), and morphological structures of oil palm. Heat Ratio Method (HRM) is one of the methods that has been successfully used to measure sap flow (SF) on monocots plants, *i.e.*, oil palm (Madurapperuma *et al*., 2009). The HRM is a heat pulse method that can do direct measurements of SF *in situ*, it is relatively cheap and easily automated for continuous, high-resolution monitoring of plant water demand (Smith and Allen, 1996). HRM gauges SF rates and volumetric flow of water in xylem tissue uses a short heat pulse principle (Bleby *et al*., 2004; Burgess *et al*., 2001).

SF is defined as the flow of water in the xylem tissue. SF is also described as a flow of water or assimilates generated by soil water resistance and hydraulic conductance of the plant (Kirkham, 2014). The SF maintains the hydraulic connection between soil and atmosphere (Steppe *et al*., 2015), therefore investigations of SF characteristics can be used to estimate actual water transpiration as well as crop water requirements (Haijun *et al*., 2015; Ismanov *et al*., 2019). Several studies have shown that transpiration response to environmental variables is specific to the climate and ecosystem where plants grow (Xu and Yu, 2020). This information is crucial because it can be used to determine transpiration heterogeneity between stands (Oteino *et al*., 2017) and calculate the ecosystem water budget (Zhao *et al*., 2016).

Moreover, Zhang *et al.* (1999) stated that the effects of the environment on plant water relations could be examined by measurements of SF in conjunction with the component of water potentials (Ψ). Water potentials are fundamental for the movement of water to the leaves in the process of photosynthesis. The gradient between Ψ_{soil} and Ψ_{plant} is the driving force for soil water uptake by the plant, while the gradient between Ψ_{plant} and $\Psi_{atmosphere}$ drives the water movement from the plant to the atmosphere (Fricke, 2017; Zhang *et al*., 2017). On oil palm, water potential can be measured using a psychrometer (Yono *et al*., 2019).

Recent studies on oil palm SF using HRM to estimate transpiration have been carried out by Bayona-Rodríguez and Romero (2016); Brum *et al.* (2020); Ellsäßer *et al.* (2020); Hardanto *et al.* (2017); Merten *et al.* (2016); Niu *et al.* (2015); Röll *et al.* (2015); Santi *et al.* (2021). On the contrary, not many have observed the Ψ_{plant} of oil palm under field conditions, one of which was Suresh *et al.* (2012b). Moreover, measurement of SF and oil palm water potential was still partially done. Hence, the characteristics of oil palm water flux as a response to environment factors are still unclear.

This research employed direct-integrated measurements of SF, Ψ_{plant}, climate, and soil variables in oil palm under field conditions. In addition, this study estimated the actual daily stand transpiration and quantified environmental variables' contribution to oil palm water flux dynamics. Thus, this study was expected to provide more detailed information about primary ecological factors that control oil palm water flux.

MATERIALS AND METHODS

Study Site

The study was conducted from 21 August to 18 September 2018 in Medan, North Sumatera. The study site had a flat topography (slope of 0%-3%) and a dominant soil type of Typic Dystrudepts. Two oil palm trees (*Elaeis guineensis* Jacq.) arranged in a 9 m wide triangle were selected. Both palms were 14 years old and well maintained. The trunk height of palm No. 1 was 6.87 m, while palm No. 2 was 7.35 m. Soil texture around oil palm sample No. 1 was sandy loam with sand, silt, and clay portions of 60%, 32% and 8%, respectively. Oil palm sample No. 2 also had a similar soil texture with the proportion of sand, silt, and clay at 55%, 36% and 9%, respectively. The rainfall (RF) pattern in the study site was equatorially marked by two peaks of the rainy season in May and September (Pradiko *et al*., 2016a). The average annual RF during the period of 2013-2018 was 2164 mm yr^{-1}. Mean air temperature ranged between 27°C to 28°C, while maximum and minimum air temperatures were 38°C and 22°C, respectively. Average relative air humidity was 80%, where lower humidity was in the middle of the year (June-August). Average solar radiation (Qs) fluctuated from 13.69 to 20.07 MJ m^{-2}.

Oil palm is a monocot, and it has a non-wood lignocellulosic material (Hashim *et al*., 2011). In contrast to dicot plants, the xylem and phloem vessels of oil palm are located within a complex structure known as vascular bundle. In the trunk, vascular bundles are scattered with various densities depending on the depth and height (Darwis *et al*., 2013). Niu *et al.* (2015) stated that the vascular bundle density in palm leaf petioles was higher compared with the trunk. It is confirmed in this study (*Figure 5*). Thus, SF and water potential can be measured at the petiole.

Sap flow (SF) measurement. SF velocity measurement was calculated using the following Equations (1) and (2):

$$V_s = \frac{V_c \rho_b (c_w + m_c c_s)}{\rho_s c_s} \quad (1)$$

where,

$$V_c = bV_h + cV_h^2 + dV_h^3 \quad (2)$$

where V_s is sap velocity (cm hr^{-1}), V_c is corrected heat pulse velocity (cm hr^{-1}), V_h is heat pulse velocity (cm hr^{-1}), ρ_b is the basic density of wood (dry weight/fresh volume), ρ_s is density of water, c_w is the specific heat capacity of wood at an average air temperature of 30°C, 1260 J kg^{-1} $°C^{-1}$ (Becker and Edwards, 1999), c_s is the specific heat capacity of the water, 4182 J kg^{-1} $°C^{-1}$ (Lide, 1992), then m_c is the water content of sapwood. Sapwood properties with installed Sap Flow Meter (SFM1) were taken to estimate ρ_b and m_c. Fresh and dry weights of sapwood were gauged before and after oven drying at 60°C for 72 hr. Fresh volume was estimated by immersing the samples in distilled water following Archimedes' principle [modified from Madurapperuma *et al.* (2009)]. V_c was estimated from V_h by using b-d as the correction coefficient (Burgess *et al.*, 2001). In this study, it was assumed that $V_c = V_h$ because the wound diameter was very small [<0.17 cm; minimum wound width listed in Burgess *et al.* (2001)].

V_h was measured using SFM1 produced by ICT International Australia. SFM1 employed the HRM, which gauged the ratio of temperature increment, following the release of a pulse of heat, at points equidistant downstream and upstream from a line heater (Bayona-Rodríguez and Romero, 2016). SFM1 sensors consisted of three probes where one probe located in the middle generated a heat pulse, and the other two were positioned above and below the heater probe equipped with thermocouples. SFM sensors were installed according to standard practice provided by ICT International, including the use of a steel drill guide to ensure that holes were drilled parallel and correctly. Also, including the use of aluminium foil and plastic shield to avoid external disturbances such as Qs, air temperature, *etc.*, SFM1 was attached in the petiole where higher vessel density and homogeneity were located (Madurapperuma *et al.*, 2009). One sensor was installed at frond No. 17 of each palm (*Figure 1*). Frond No. 17 was selected to represent the intermediate value between the upper (frond No. 9) and lower frond (frond No. 25) (Bayona-Rodríguez and Romero, 2016). Frond addition of sampled palms was just at only one frond per month (data not shown); thus, it was assumed that there was no change in fronds number. The heat pulse used was 30 J. The selection of heat pulse levels depends on environmental conditions and the plant's transpiration rate. If during the measurement there is a diagnostic comment, such as 'temperature rises insufficient' then the heat pulse must be increased. But it should be noted that plant tissue could be damaged when the heat pulse level is too high. As a comparison, Bayona-Rodríguez and Romero (2016) used 35 J in similar research conducted previously.

Volumetric SF (Q) was calculated by multiplying V_s with the total area that actively transpires (A) the sap of each petiole near SFM1 attached. 'A' was estimated by multiplying the area and the total number of active vascular bundles. The images of the petiole were processed using ArcGIS 10 to measure the total petiole area, as well as the number and total area of the active vascular bundles. The calculation of the active vascular bundles only addressed the vascular bundles that transpired a safranin solution (*Figure 5*).

Measurement of Frond Water Potential

The frond water potential of the sample palms was measured using a psychrometer (PSY1) produced by ICT International Australia. PSY1 can log changes in plant water status/potential continuously; thus, the data logged by PSY1 directly reflect the energy required to access water (Dixon and Downey, 2013). PSY1 was attached to the petiole of frond No. 17 and maintained using the procedures by Tran *et al.* (2015). PSY1 was placed in the front part of the petiole, while the SFM1 was installed in the back part of the petiole. PSY1 was installed 20 cm away from SFM1, as illustrated in *Figure 1*. Heat pulse velocity (cm hr^{-1}) and frond water potential/ Ψ_{frond} (MPa) data were logged every 15 min during 29 days of observation.

Measurement of soil and climate variables. Observation of soil physical properties included bulk density (g cm^{-3}), porosity (%), permeability (cm hr^{-1}), and soil moisture (SM) (%). For these properties, undisturbed soil samples were collected using a core/ring sampler at the radius of 50 cm, 100 cm, 150 cm and 200 cm from the basal stem. Bulk density was calculated based on the dry weight of the soil and the volume of the ring sampler. Then, porosity was determined from the bulk and particle densities. The particle density was obtained from the ratio of the soil dry weight to soil volume. A pycnometer was employed to calculate soil volume. Meanwhile, the permeameter calculated the permeability. Furthermore, Soil Moisture Meter (SMM) MP 306 was installed at the same radius of soil sampling (*Figure 1*).

RF (mm), air temperature (°C), relative humidity

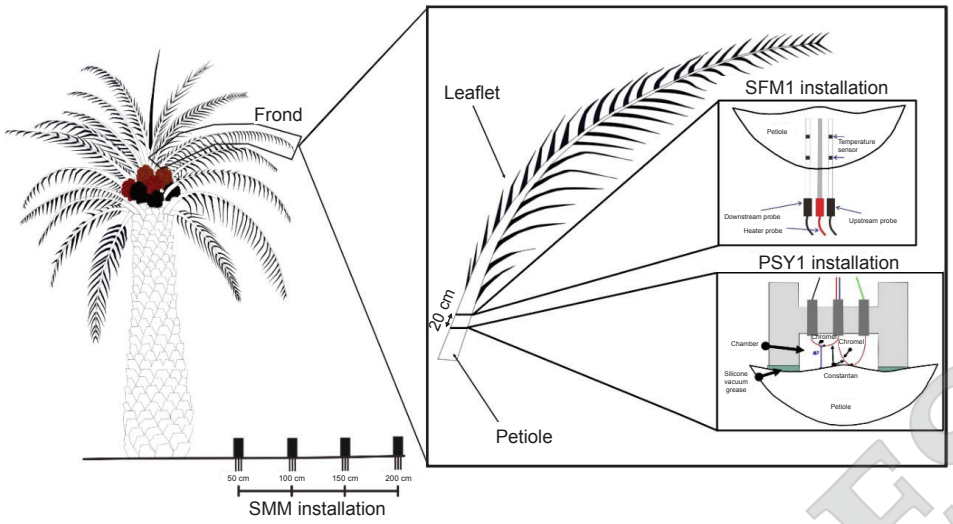

Figure 1. Installation of SFM1, PSY1, and SMM on the plotted palms.

(%), and Qs (W m^{-2}) were gauged by AWS Davis Vantage Pro-II Plus. The data logging interval of AWS was formatted every 15 min and the same for SFM1, PSY1, and SMM. Vapour pressure deficit (VPD) was estimated from air temperature and relative humidity using an equation postulated by Murray (1967). Daily Qs (MJ m^{-2} d^{-1}) was calculated from the quarter-hourly of Qs (W m^{-2}) based on the following Equation (3):

$$Qs.d = \frac{\Sigma\,(G_{15} \times \text{logging periods})}{1\,000\,000} \quad (3)$$

where, $Qs._d$ is daily Qs (MJ m^{-2}), $Qs._{15}$ is Qs per 15 min (W m^{-2}), logging periods is 15 min or 900 s.

Data analysis. The daily volumetric SF was cumulated to estimate the total daily transpiration. The multiple linear regression method was employed to determine the effects of Ψ_{frond}, SM, RF, Qs, and VPD on SF dynamic. A similar method was also used to quantify the effects of climate (RF, Qs, and VPD) and SM on Ψ_{frond}. According to Ismanov *et al.* (2019) and Cai *et al.* (2020), gradients of water potential on the soil-plant-atmosphere continuum (SPAC) are a driving force for SF and transpiration.

Data analysis also included quantification of the contribution of Ψ_{frond}, SM, RF, Qs, and VPD to the dynamic of SF. Furthermore, the contribution of SM, RF, Qs, and VPD to Ψ_{frond} fluctuations was also quantified. Quantification of the contribution of each variable to SF and Ψ_{frond} was estimated using a computer-intensive relative importance metric developed by Lindemann, Merenda, and Gold (known as metric LMG) (Grömping, 2006; 2015; Lindemann *et al.*, 1980). The metric LMG was calculated using R-software version 4.0.4 and RStudio version 1.4.1106, where its calculation package or the package relaimpo was obtained from the following website: http://prof.beuth-hochschule.de/groemping/software/relaimpo/.

Moreover, the effects of environment variables that have a major contribution to the SF rate (cm^3 hr^{-1}) and Ψ_{frond} were analysed diurnally using a hysteresis curve. The hysteresis curve is commonly used to identify the responses of SF and Ψ_{frond} to environment variables. Analysis using the hysteresis curve was employed in this study because, in a diurnal pattern, changes in environment variables in the morning will result in a different pattern compared to that in the mid-day (Roddy *et al.*, 2013). In this study, plot points in the hysteresis curve were divided into three time zones, they were before dusk (24.00-06.15), daytime (06.30-18.45), and after dawn (19.00-23.45). In this study, the hysteresis of SF and frond was expressed by the area inside the curve or loops.

RESULTS AND DISCUSSION

Soil and Climate Variables Condition

Soil physical properties around sampled palms are shown in *Table 1*. It indicates that soil bulk density increased from the most outer radius to the most inner radius. On the contrary, soil porosity and soil permeability decreased from the most outer radius to the most inner radius.

TABLE 1. SOIL'S PHYSICAL PROPERTIES AT DIFFERENT RADIUS OF 50, 100, 150, AND 200 CM FROM THE BASAL STEM

Radius (cm)	Bulk density (g cm^{-3})	Porosity (%)	Permeability (cm hr^{-1})
50	1.53 ± 0.02	44.05 ± 0.73	0.22 ± 0.09
100	1.40 ± 0.04	49.05 ± 1.75	0.27 ± 0.03
150	1.32 ± 0.04	52.04 ± 1.98	0.52 ± 0.07
200	1.25 ± 0.07	55.04 ± 1.30	0.55 ± 0.03

Note: Soil samples were collected twice in weeding circle of each palm. SE is the standard error.

Figure 2 shows SM (%vwc), RF (mm), Qs (W m^{-2}), and VPD (kPa) during the study. SM at a radius of 200 cm is the highest compared to another radius. The SM pattern followed the pattern of other soil physical properties. The highest SM is found in the soil with lower bulk density, higher porosity, and higher permeability. A previous study showed that soil physical properties in the weeding circle affected SM, where the highest value of average SM was found in the radius of 200 cm (Pradiko *et al.*, 2020).

Furthermore, it has been raining more for the last 15 days of the study. Most of the RF occurred in the afternoon to evening. Therefore, it implied a lower VPD value while Qs was relatively unaffected.

SF Characteristics

SF measurement during the study is shown in *Figure 2*. Overall, SF in both sample plants did not exceed 800 cm^3 hr^{-1}. The SF is similar to Qs and VPD, which is low at night and then peaks during the day. Meanwhile, there is no clear pattern between SF and other environmental variables.

Based on the multiple linear regression analysis, Ψ_{frond} and environmental factors (RF, Qs, VPD, and SM) explained 80.02% and 76.59% of the SF on plant samples No. 1 and 2, respectively. The results are similar to the research conducted by Xu and Yu (2020) on arid and semi-arid ecosystems showing that Qs and VPD are two of three climatic factors besides air temperature that can explain 77.00% to 84.00% of variations in plant SF. Qs and VPD had a major contribution to the SF, which can be seen from the higher value of contribution (%) and correlation coefficient (r) in *Table 2*. VPD explains 33.73% and 25.72% palm 1 and 2 SF dynamics, respectively. The correlation between Qs and SF, as well as VPD and SF, is more than 0.60. Therefore according to Obilor and Amadi (2018), it is classified as significantly strong. Moreover, Qs explain SF dynamic is higher than VPD. Qs also has a considerably stronger correlation to SF than VPD. It means Qs is more dominant in affecting the SF than VPD. Therefore, Qs is more prevalent in affecting the transpiration of oil palm. It is related to research conducted by Xu and Yu (2020) which shows Qs is an environmental factor that acts as the primary driving force for SF.

The findings in this study were different from the research by Bayona-Rodríguez and Romero (2016), which stated that the daily fluctuation of SF depended on weather variations, especially VPD. Brum *et al.* (2020) also noted that VPD assigned more influences on transpiration than PAR (Photosynthetic Active Qsiation). Meanwhile, in another study, Röll *et al.* (2015) stated that transpiration was related to VPD and Qs, though it was unclear which one was more dominant in affecting SF.

Figure 3a shows that the SF rate started to increase at 06:30 am and reached the peak at 00:45-1:00 pm. Average SF at the peak was 386.77 cm^3 hr^{-1} and 457.79 cm^3 hr^{-1} on palm samples No. 1 and 2, respectively. Furthermore, SF tended to plateau and then started to decrease after 3:00 pm. Results of this study were different from the other studies, which described that daily transpiration of oil palm reached the peak at 10:00-11:00 am, it was before maximum Qs (12:00 am-1:00 pm), and when VPD reached the peak (2:00-3:00 pm) (Röll *et al.*, 2015).

Meanwhile, a previous study reported a relatively similar pattern of SF fluctuation using a five-year-old oil palm in Colombia. In that study, the SF rate on oil palm started to increase at 07.30 am, peaked by mid-day, and decreased after 3:50 pm (Bayona-Rodríguez and Romero, 2016). However, the pattern of SF in this study was relatively similar to those in other studies using different plants, *i.e.*, poplar (Zhang *et al.*, 1999), banana (Haijun *et al.*, 2015), and black locust (Zhang *et al.*, 2018).

The plot between quarter-hourly stand SF against Qs and VPD shows clockwise hysteresis loops (*Figure 3b*). The same pattern was observed in hardwood forests (Matheny *et al.*, 2014) and plants in arid and semi-arid ecosystems (Xu and Yu, 2020). The difference in response of SF to the environment before dusk, during the daytime, and after dawn can be seen in the hysteresis loops. During the daytime, the SF rate tended to increase along with the increment of VPD. However, when VPD was higher than 1 kPa, there was no further dramatic increase in transpiration rate; even the SF decreased when VPD was 2.1 kPa. These findings were similar to the previous studies that described a decrease in transpiration of oil palm when VPD was 1.7-2.0 kPa (Carr, 2011; Meijide *et al.*, 2017; Waite *et al.*, 2019). A decrease in transpiration rate is closely associated with stomatal conductance (g_s), where the high value of VPD (Hernandez *et al.*, 2016; Ocheltree *et al.*, 2014; Su *et al.*, 2019) or Qs (Francesconi *et al.*, 1997; Massonnet *et al.*, 2007) cause a depression in the stomatal conductance. Li *et al.* (2019a) added that the concentration of phytohormones, *i.e.*, abscisic acid (ABA), in leaf was correlated positively with the sensitivity of stomata conductances to VPD. It

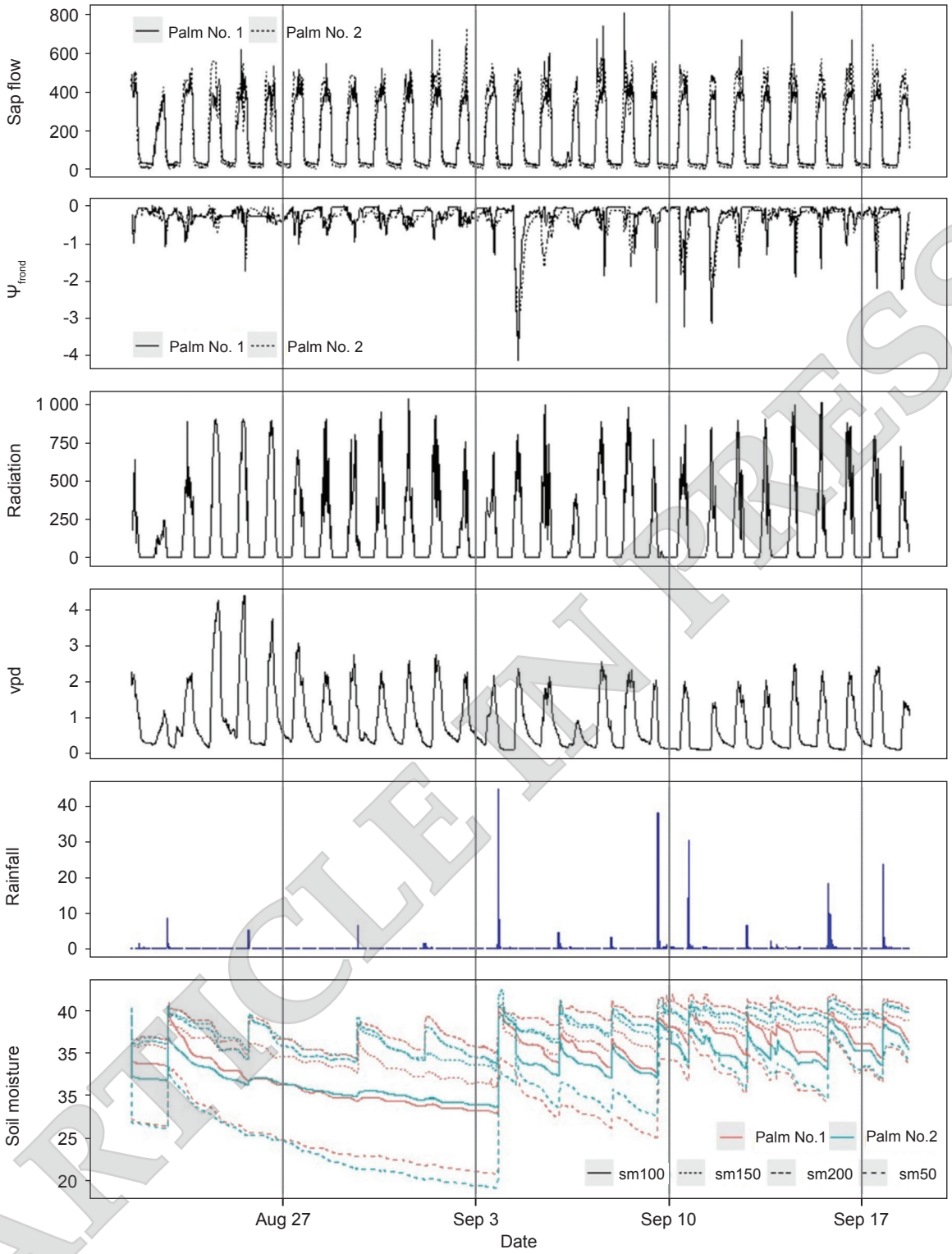

Figure 2. Qs (W m^{-2}), VPD (kPa), RF (mm), SM (%), daily Ψ_{frond} (MPa) and SF (cm^3 hr^{-1}) of frond No. 17 during the observation. SM_{50}, SM_{100}, SM_{150}, and SM_{200} are SM at a radius of 50 cm, 100 cm, 150 cm and 200 cm from the basal stem, respectively.

is unclear whether stomata conductance is a direct response of oil palm to environmental stress or is mediated by a chemical reaction or another signal stress (Waite *et al.*, 2019). In another study, it stated that the stomatal aperture could be regulated by sugars and sugar-derived molecules (Figueroa and Lunn, 2016); water status, turgor, and ABA concentration (Brodribb and McAdam, 2017); CO_2 concentration in ambient air and intercellular air spaces (Engineer *et al.*, 2016).

The SF-hysteresis curve as a function of Qs showed a similar clockwise pattern (*Figure 3c*) to that in *Figure 3b*. An identical pattern was obtained in hysteresis loops between sap flux

TABLE 2. THE CONTRIBUTION AND PARTIAL PEARSON CORRELATION OF VARIABLES TO SAP FLOW (SF)

Variables	Palm 1		Palm 2	
	Contribution (%)	r	Contribution (%)	R
Ψ_{frond}	7.90	-0.46**	8.05	-0.45**
VPD	33.73	0.83**	25.72	0.75**
RF	0.17	-0.08**	0.22	-0.08**
Qs	35.63	0.84**	40.43	0.85**
SM_{50}	0.49	-0.12**	0.37	-0.10**
SM_{100}	0.58	-0.15**	0.55	-0.15**
SM_{150}	0.56	-0.16**	0.63	-0.15**
SM_{200}	0.96	-0.18**	0.60	-0.14**
Total	80.02		76.59	

Note: The contribution (%) was calculated using the metrics LMG (Grömping 2006; 2015).
The total contribution is equal with R^2 of variables to SF.
Ψ_{frond} - frond water potential; VPD - vapour pressure deficit; RF - rainfall; Qs - solar radiation; SM_{50-200} - soil moisture at radius 50 cm, 100, 150 and 200 from basal stem.
**correlation is significant at the 0.01 level (1-tailed).

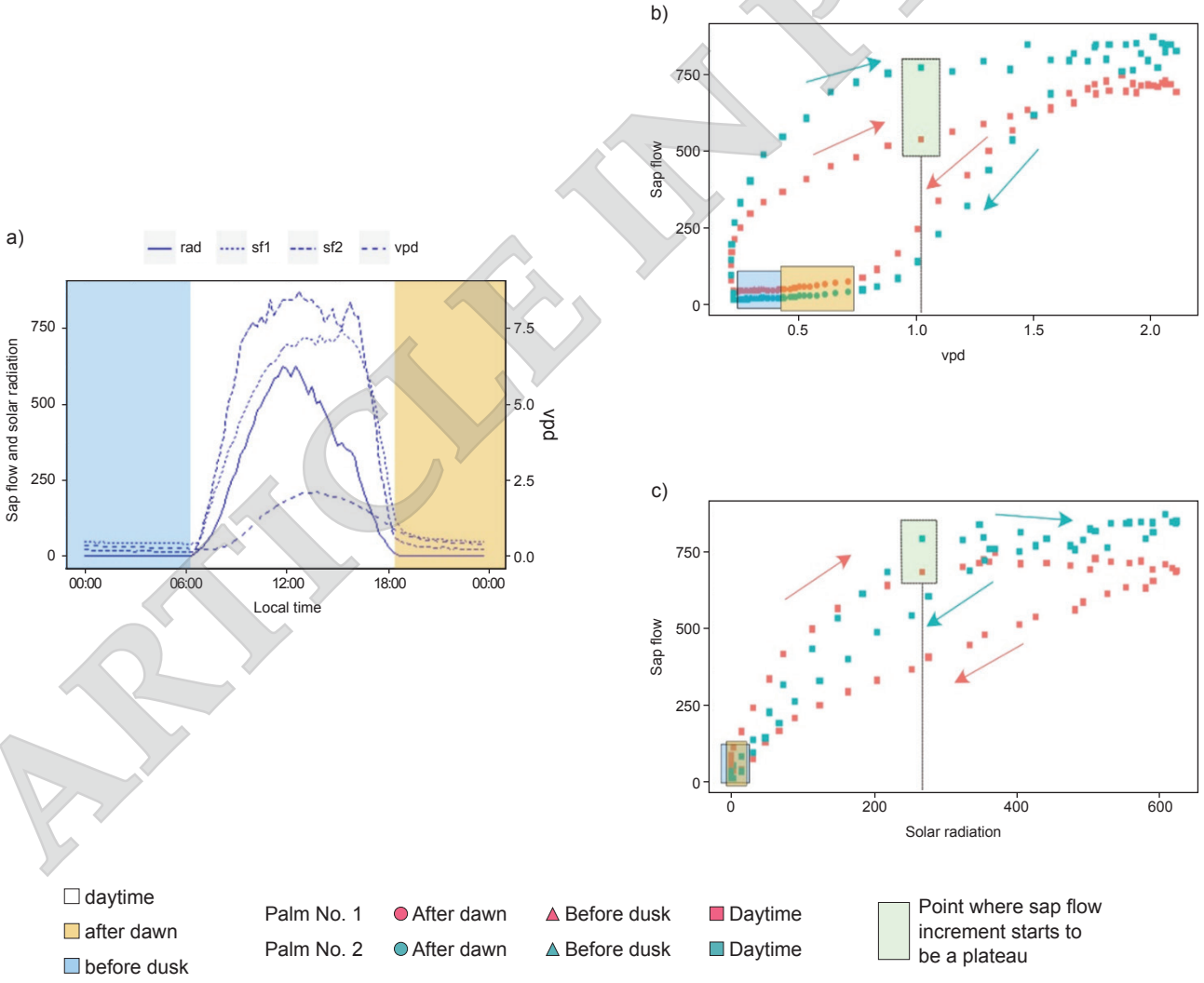

Figure 3. Fluctuation of SF, Qs, and VPD in every 15 min (a) Hysteresis curve of SF as a function of Qs and VPD (b and c). SF (cm³ hr⁻¹), Qs (W m⁻²), VPD- vapour pressure deficit (kPa). Arrows in Figures 3b *and* 3c *indicated the progression of the diurnal cycle from sunrise to sunset. The data in the yellow box shows the conditions after dawn, while the data in the blue box shows the conditions before dusk. Box in the black dashed vertical line is a point where the increment of SF rate starts to be a plateau. The detail of average and standard deviation SF, Qs, and VPD data from* Figure 3a *came from the average of all-day data.*

and Qs by Xu and Yu (2020). The data of sap flux response to Qs at night, where there is no light, are low and concentrated in the bottom-left of the curve. During the daytime, the SF rate drastically increased until solar was 267 W m^{-2}; then the SF tended to be stagnant. SF then decreased after Qs was 622 W m^{-2}. These findings were different from the study by Brum *et al.* (2020), which described that decrease in the rate of sap flux density on oil palm occurred when the value of PAR was 600 µmol m^{-2} s^{-1} or 130 W m^{-2} (assumed 1 W m^{-2} = 4,6 µmol m^{-2} s^{-1}) and VPD was more than 1 kPa. Meijide *et al.* (2017) also stated that mature oil palm reached maximum transpiration when PAR was 600 µmol m^{-2} s^{-1}.

Figures 3b and *3c* show that the SF rate is lower in the period after sunset to the time before sunrise. Another interesting fact from the hysteresis curves is that the SF after dawn is slightly higher than before dusk. These conditions indicate that plants are trying to replenish water loss in plants during daytime transpiration (Xu and Yu, 2020). The SF at night reveals the presence of night-time transpiration. The respiration causes night-time transpirational water loss at night. This process can provide more efficiency in using water for leaf expansion (Fricke, 2019). A gradual decrease of the hysteresis curve between SF and VPD before dusk and after dawn indicates that the VPD is involved in regulating night-time transpiration. A previous study on Eucalyptus plants showed that VPD and wind speed were factors that drive nocturnal transpiration (Phillips *et al.*, 2010).

Based on the response of the SF rate to VPD and Qs conditions, this study concludes that the SF rate reached the plateau point at VPD of 1 kPa and Qs of 267 W m^{-2}. Dufrene and Saugier (1993) explained that there was no significant change in stomatal conductance and net rate of CO_2 uptake after PAR exceeded 1100 µmol m^{-2} s^{-1} (equal to 239 W m^{-2}) at VPD of 1 kPa. Cheah and Teh (2020) obtained the light saturation for stomatal conductance at about 1500 µmol m^{-2} s^{-1} (equal to 326 W m^{-2}). The plateau point here was defined as a point where the increment in VPD and Qs did not drastically increase the SF rate.

Although this research shows that Qs affect SF more, different combinations of Qs and VPD conditions will affect the SF differently. There is a complex relationship between Qs and VPD in influencing SF dynamics. Qs and VPD had a significant combined effect on SF (Matheny *et al.*, 2014). Thus, further study is needed to understand how these factors the affect SF of oil palm. According to Apichatmeta *et al.* (2017), a mature oil palm would reach optimum photosynthesis at a PAR value of 600 µmol m^{-2} s^{-1} without describing its association with VPD. Meanwhile, Meijide *et al.* (2017) reported that transpiration of oil palm started decreasing when the PAR had not reached the maximum point. At this point, stomata had partially closed due to leaf-level water stress initiated by VPD and PAR (Waite *et al.*, 2019). Brum *et al.* (2020) described sap flux which reached the highest point before the maximum value of PAR, showing that the physiological condition of oil palm was more affected by atmospheric water stress than light availability.

Factors Affecting Frond Water Potential

The frond was negatively correlated to the SF (*Figure 2*), with the value of partial Pearson correlation being negatively moderate (*Table 2*). Ψ_{frond} reached the minimum at mid-day (*Figure 5a*), it agreed with the previous study by Suresh *et al.* (2012b). In detail, Ψ_{frond} has the minimum values at about 30-45 min after SF reached the maximum value. The minimum value of Ψ_{frond} on palm samples No. 1 and 2 was -0.84 and -0.78 MPa, respectively. The leaf water potential decreased in the mid-day while the SF increased (Beyer *et al.*, 2018; Zhang *et al.*, 1999). Thus, when the Ψ_{frond} was more negative, the potential gradient between plant and environment would be more significant, and then the SF rate would be higher (Cai *et al.*, 2020).

Analysis of the determination coefficient showed that Ψ_{frond} fluctuation was only able to explain 7.90% of SF fluctuation on palm No. 1 and 8.05% on palm No. 2. It indicates that measurement of Ψ_{frond} solely is insufficient to explain SF dynamic because SF movement is a function of water potential gradients between the SPAC, as stated in the previous study by Steppe *et al.* (2015). A more complete water potential observation (not only in the frond) will determine the relationship between water potential and transpiration. For example, Wang *et al.* (2013) research showed that the potential difference between root and leaf showed a significant relation with transpiration. Furthermore, a study conducted by Zhang *et al.* (2014) showed that the condition of the leaf-root-soil water potential would significantly affect the plant's evapotranspiration.

Plant water potential (represented by Ψ_{frond}) was affected by variables of climate, soil, and condition of the plant (Wang *et al.*, 2013). Quantification of Ψ_{frond} response to climate and soil variables is listed in *Table 3*. The analysis using the LMG Method showed that the effects of climate and soil variables on Ψ_{frond} were not higher than 24%. Climate variables consistently had more impacts on Ψ_{frond} than SM. A similar condition was found in *Robinia pseudoacacia*, where leaf water potential values were more affected by air temperature, air humidity, and Qs than soil temperature (Wang *et al.*, 2013).

Qs and VPD are two variables with the highest

values of partial Pearson correlation to Ψ_{frond}. Coolong *et al.* (2012) stated that Ψ_{frond} was well correlated with air temperature, humidity, dew point, and Qs. Nevertheless, VPD only represented 8.53% and 8.39% of Ψ_{frond} fluctuation on palms No. 1 and 2, respectively. Meanwhile, Qs only explained 9.21% and 7.57% of Ψ_{frond} flux on palm samples No. 1 and 2, respectively. There was no consistent contribution of Qs and VPD to the dynamics of Ψ_{frond} on the two plant samples. Therefore the contribution pattern of the two variables on Ψ_{frond} remained unclear.

The less contribution of the environment to the Ψ_{frond} dynamics in this study is related to the complexity of SPAC. Changes in environmental conditions will affect the plant, soil and atmospheric water potential. Therefore, to improve understanding of the water potential dynamic, it is better to simultaneously measure the soil-plant-atmosphere water potential. In addition, the oil palm stem plays a significant role in diurnal water flux by storing water (Waite *et al.*, 2019) and large amounts of carbohydrates to buffer environmental influences (Legros *et al.*, 2009; Suresh *et al.*, 2012b). Therefore, not all ecological changes will immediately affect the dynamics of Ψ_{frond}.

Figures 4a and *4b* reveal that Ψ_{frond} were more negative as Qs and VPD increased. Then, Ψ_{frond} tended to increase drastically to about -0.1 MPa after dawn until dusk. *Figures 4c* and *4d* show the clockwise hysteresis loops. Both figures show that Ψ_{frond} after dawn is lower (more negative) than before dusk. This condition is in line with the pattern of SF response to Qs and VPD. Moreover, Ψ_{frond} reached the minimum value at the mid-day when the VPD value was 2.1 kPa and Qs reached the value of 622 W m^{-2}.

Oil palm is an isohydric plant. It can maintain a more or less constant midday leaf water potential regardless of variations in atmospheric conditions and predawn soil water potential (Hochberg *et al.*, 2018; Martínez-Vilalta and Garcia-Forner, 2017). Isohydric plants are characterised by flatter slopes between predawn and midday water potential (Charrier, 2020; Villalobos-González *et al.*, 2019). The slope between predawn and midday water potential in this study is 0.915 (less than 1 - data not shown), indicating that oil palm is an isohydric species. Consequently, to avoid hydraulic failure, oil palm plants develop considerable plasticity in the hydraulic system, develop embolic resistance from environmental conditions, and take advantage of the large stem capacitance (Waite *et al.*, 2019).

Effects of RF and SM on SF and Ψ_{frond}

In comparison to other variables, RF and SM were not dominant in affecting SF and Ψ_{frond}. A similar result was found in the previous research on black locusts by Zhang *et al.* (2018), where RF and SM were not correlated to the daily stand transpiration. The less contribution of RF was because it did not directly affect SF and Ψ_{frond}. However, it affected Qs, VPD, and SM. RF might decrease Qs and VPD as well as increase SM (Li *et al.*, 2019b). More detailed studies on the effects of RF and SM at several radius in an oil palm weeding circle had been reported by Pradiko *et al.* (2020), where there was a strong and positive correlation between RF and SM.

The results are different from previous studies, which showed a significant SF response to SM as in the study of Ismanov *et al.* (2019); Sitková *et al.* (2014); Zha *et al.* (2017). SM also did not contribute much to Ψ_{frond}. In contrast, other studies explain that SM also plays a vital role in the dynamics of leaf water potential (Rivera-Méndez *et al.*, 2012). *Figure 3* shows that SF and Ψ_{frond} fluctuations do not follow SM changes. For example, SF and Ψ_{frond} tend to be constant even though there was a decrease in SM from 27 August to 4 September. The day after, midday Ψ_{frond} was observed to reach its lowest value on palm samples No. 1 and 2, *i.e.*, -3.58 MPa and -4.13 MPa, respectively. The

TABLE 3. THE CONTRIBUTION AND PARTIAL PEARSON CORRELATION OF VARIABLES TO Ψ_{frond}

Variables	Palm No. 1		Palm No. 2	
	Contribution (%)	r	Contribution (%)	r
VPD	8.53	-0.37**	8.39	-0.37**
RF	0.03	-0.03	0.05	-0.10
Qs	9.21	-0.40**	7.57	-0.37**
SM_{50}	1.37	-0.10**	5.02	-0.12**
SM_{100}	0.86	-0.07**	1.03	-0.04**
SM_{150}	1.35	-0.03	1.12	-0.03
SM_{200}	0.29	-0.02	0.65	-0.05
Total	21.65		23.83	

Note: The contribution (%) was calculated using the metrics LMG (Grömping 2006; 2015). The total contribution is equal with R^2 of variables to Ψ_{frond}. VPD - vapour pressure deficit; RF - rainfall; Qs - solar radiation; SM_{50-200} - soil moisture at radius 50 cm, 100, 150, and 200 from basal stem. **correlation is significant at the 0.01 level (1-tailed).

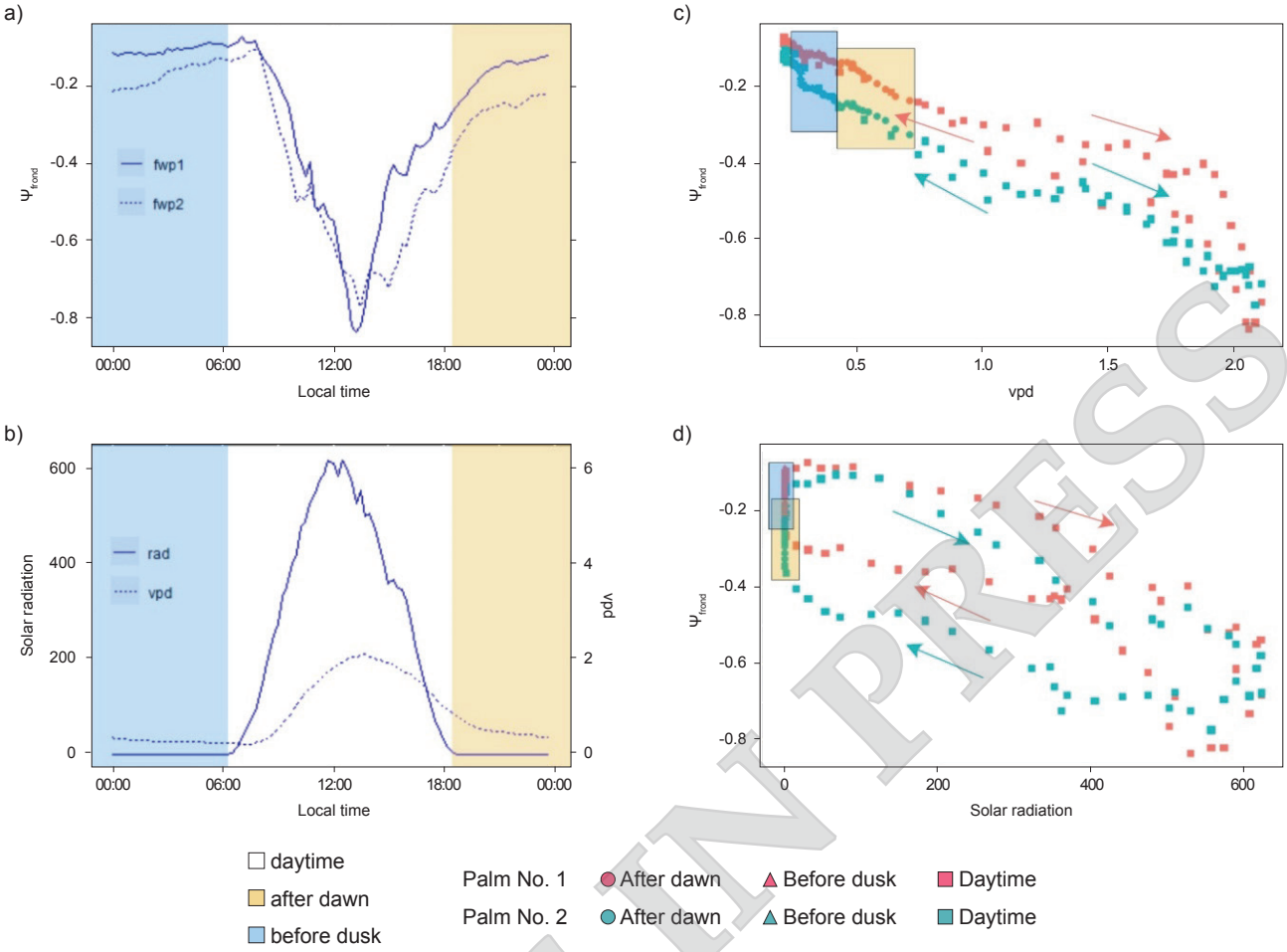

Figure 4. The quarter-hourly data of frond water potential (Ψ_{frond}) (a), VPD and Qs (b). Hysteresis curve for average values of frond water potential as a function of the VPD and Qs (c dan d). fwp1: frond water potential of palm No. 1 (MPa), fwp2: frond water potential of palm No. 2 (MPa), rad: Qs (W/m^2), vpd: vapour pressure deficit (kPa). The arrows in Figures 4c *and* 4d *indicated the progression of the diurnal cycle from sunrise to sunset. The data in the yellow box shows the conditions after dawn, while the data in the blue box shows the conditions before dusk. The details of average and standard deviation frond water potential, Qs as well as VPD data from* Figure 4a *came from the average of all-day data.*

SF value during the plateau phase also tends to be lower than the previous days. The same thing also happened in the period 5-9 September, where Ψ_{frond} did not immediately respond to the decline in SM. Instead, the Ψ_{frond} reduction was observed on 10-11 September. The lag, especially between the decrease in SM and Ψ_{frond}, ensures that oil palm has a specific capacitance in buffering environmental changes.

SM contribution to SF fluctuation was different when compared to Ψ_{frond}. The contribution of SM to SF followed the order of $SM_{200} > SM_{100} > SM_{150} > SM_{50}$ (*Table 2*), and the order was $SM_{50} > SM_{150} > SM_{100} > SM_{200}$ for the contribution of SM to Ψ_{frond} (*Table 3*). This study indicated that SM at the edge of the weeding circle tended to have more influence on SF than those at the other radius. The pattern of SF response to SM was regulated by roots distribution because tertiary and quaternary roots, which have a significant role in water and nutrient uptake, were dominantly found at >150 cm from the basal stem (Pradiko *et al.*, 2016b). However, the contribution pattern of SM to the Ψ_{frond} is difficult to explain. Aside from buffer effects, the absence of drought and drastic changes in SM during the study allegedly caused the contribution of SM to water flux (especially Ψ_{frond}) to be minimal. Waite *et al.* (2019) stated that oil palm growing in riparian areas has lower xylem water potential than in well-drained areas. Therefore, it is necessary to conduct further research in drier areas to ascertain the role of SM in Ψ_{frond}.

Oil Palm Transpiration

As explained before, the SF needs to be multiplied by the area of the active vascular bundles to obtain the oil palm stand transpiration. The density of vascular bundles in the petiole of the two palms is shown in *Figure 5*. It shows that the vascular bundles spread across the entire cross-section, where more vascular bundles are

located near the bark of the petiole. The total area of active vascular bundles for palm samples No. 1 and 2 are 31.890 cm^2 (78.49% of total petiole area) and 34.350 cm^2 (83.36% of total petiole area), respectively. It should be understood that the calculation of vascular bundles is critical so that the estimation of oil palm stand transpiration is not overestimated.

Stand transpiration of the oil palm in this study is shown in *Figure 6*. The daily stand transpiration ranged between 0.83-1.53 mm day^{-1} and 0.82-1.66 mm day^{-1} on the oil palm samples No. 1 and 2, respectively. Furthermore, average transpiration was 1.28 dan 1.39 mm day^{-1} on palm trees No. 1 and 2, respectively. The pattern of daily transpiration of the two palms nearly followed the daily fluctuation of Qs and VPD. The low daily transpiration occurred when the daily Qs were less than 10 MJ m^{-2} day^{-1} and the average VPD was less than 0.5 kPa. Though the daily transpiration increased along with the increment of Qs and VPD, it tended to be stagnant when the Qs were higher than 15 MJ m^{-2} day^{-1}, and the average VPD was higher than 1.0 kPa.

At least for four days, stand daily transpiration was lower than on any other day (*Figure 6*). The combination of Qs and VPD is a significant contributor to this situation. However, there is also an indication that decreasing Ψ_{frond} due to the drop in SM at 1-2 days earlier has a role in lowering stand daily water loss (*Figure* 3). SM may have a more significant contribution in determining daily transpiration in drier areas, such as the southern part of Indonesia (Darlan *et al.*, 2016). Research conducted by Sitková *et al.* (2014) on European beech showed that sap flux would decrease by up to 30% compared to well-irrigated areas under drought stress conditions.

Compared to other previous studies, the transpiration of the 14 years old oil palm in this study was higher than the younger palm. Bayona-Rodríguez and Romero (2016) estimated that transpiration of five years old oil palm was 1.15 mm day^{-1}. Moreover, transpiration of 12 years old oil palm was 1.1 mm day^{-1} by Niu *et al.* (2015) and 2.5 mm day^{-1} by Röll *et al.* (2015). In this study, the stand transpiration of oil palm was relatively similar to the other crops. In comparison, transpiration of rubber was 2.44 mm on day^{-1} (Kobayashi *et al.*, 2014), cacao under different shade tree shelters was about 0.5-2.2 mm on day^{-1} (Kohler *et al.*, 2014), reforestation and agroforestry stands were about 0.6-2.5 mm day^{-1} (Dierick *et al.*, 2010), and the tropical forest was about 1.0-1.7 mm day^{-1} (McJannet *et al.*, 2007).

Assumed that evapotranspiration of oil palm was about 4.7 mm day^{-1}, it was estimated that transpiration of oil palm in this study comprised about 30% of the stand evapotranspiration. A previous study stated that the transpiration of oil palm included about 8%-53% of total evapotranspiration. The remaining 70% component of the evapotranspiration was the evaporation of the soils and other vegetations on the soil surface. In addition, the trapped water on the leaves petioles might have contributed to the evapotranspiration of oil palm (Röll *et al.*, 2015).

Information about the daily stand transpiration supports oil palm agricultural practices, especially water management. The results can be used for model development to estimate oil palm water requirements and apply water conservation in oil palm plantations. Water conservation is essential to conserve excess water in the rainy season and improve SM in the dry season. High SM in the dry season, where Qs and VPD are pretty high, can increase oil palm productivity (Brum *et al.*, 2020). Several techniques to conserve water in an oil palm plantation, such as silt pit, ridge terrace, or cover crops (Ariyanti *et al.*, 2016). Bare soil should be avoided on the plantation's floor because it can elevate water losses from the ground due to the evaporation process and make the soil vulnerable to erosion and nutrient leaching (Satriawan *et al.*, 2021).

CONCLUSION

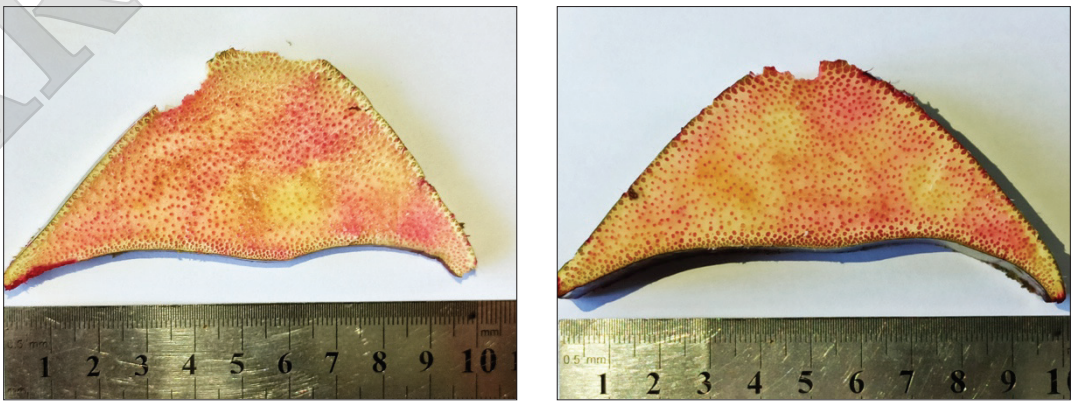

Figure 5. A bottom-up view of the petiole segment from sample palm No. 1 (left) and palm No. 2 (right) after soaking in a container of 1% safranin solution and left to transpire for 72 hr. Some parts were damaged during the preparation of the sample.

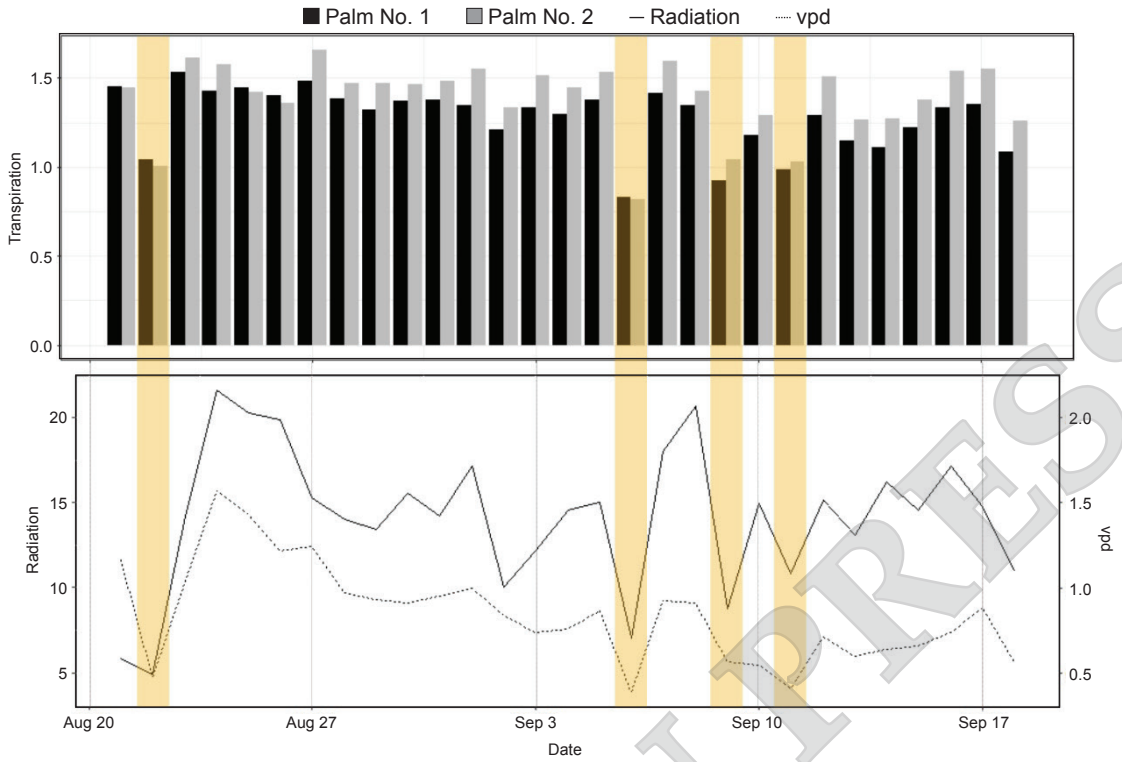

Figure 6. Stand transpiration of the oil palm during the study. The low values of Qs (Qs) and VPD at the beginning of the study were caused by the process of data recording that started at 00:30 pm local time. Transpiration was calculated using SF rate that was measured using HRM. Assumed that the oil palm had 40 fronds and the radius of the canopy was 2.5 m. Unit of the transpiration, Qs, and VPD was mm day^{-1}, MJ m^{-2} day^{-1}, and kPa, respectively. The area highlighted in yellow was the low stand transpiration when the Qs was <10 MJ m^{-2} day^{-1} and or VPD was <0.5 kPa.

This study showed that SF on oil palm increased after 06:30 am, reached the peak by mid-day, tended to be a plateau until 03:00 pm, and then decreased thereafter. Environment variables that had a major contribution in affecting SF were Qs > VPD > SM > RF. Frond water potential (Ψ_{frond}) was negatively correlated to the SF. However, the measurement of only Ψ_{frond} may not be sufficient to understand the SF movement in oil palm, it needs to be accomplished with the data of gradient of water potential in the continuum of soil-plant-atmosphere.

Frond water potential decreased as the SF increased, it reach the minimum value when the SF reached the maximum value. Environment variables that had a major contribution to the Ψ_{frond} were Qs and VPD. However, the contribution of environmental variables to the Ψ_{frond} fluctuation was not as high as their contribution to the dynamics of SF. This indicated that changes in environmental conditions might cause more impacts on atmospheric water potential ($\Psi_{atmosphere}$), so there would be changes in gradient potential between $\Psi_{atmosphere}$ and Ψ_{frond} that decrease or increase the SF rate.

This study also revealed that daily stand transpiration of the 14 years old oil palm estimated by SF measurement was about 0.82-1.66 mm day^{-1}. The stand transpiration comprised about 30% of the stand evapotranspiration. Data of stand transpiration are useful for improving agronomic practices, especially in water management.

ACKNOWLEDGEMENT

The authors are grateful for all the support from the Indonesian Oil Palm Research Institute (IOPRI), colleagues, technicians, and reviewers in preparing this article. Moreover, we would also like to thank PT Labodia Prima as the sensors provider.

REFERENCES

Apichatmeta, K; Sudsiri, C J and Ritchie, R J (2017). Photosynthesis of oil palm (*Elaeis guineensis*). *Sci. Hortic.*, *214*: 34-40. DOI: 10.1016/j.scienta.2016.11.013.

Ariyanti, M; Yahya, S; Murtilaksono, K; Suwarto and Siregar, H H (2016). Water balance in oil palm plantation with ridge terrace and *Nephrolepis biserrata* as cover crop. *J. Tropical Crop Sci.*, *3(2)*: 35-41.

Bayona-Rodríguez, C J and Romero, H M (2016). Estimation of transpiration in oil palm (*Elaeis guineensis* Jacq.) with the heat ratio method. *Agron.*

Colomb., *34(2)*: 172-178. DOI: 10.15446/agron.colomb.v34n2.55649.

Becker, P and Edwards, W R N (1999). Corrected heat capacity of wood for sap flow calculations. *Tree Physiol.*, *19*: 767-768.

Beyer, R; Pretzsch, H and Cournède, P H (2018). The co-regulatory interaction of transpiration and water potential, and implications for stomatal conductance models. *bioRxiv*. p. 1-10. DOI: 10.1101/237826.

Blatt, M R; Chaumont, F and Farquhar, G (2014). Focus on water. *Plant Physiol.*, *164*: 1553-1555. DOI: 10.1104/pp.114.900484.

Bleby, T M; Burgess, S S O and Adams, M A (2004). A validation, comparison and error analysis of two heat-pulse methods for measuring sap flow in *Eucalyptus marginata* saplings. *Funct. Plant Biol.*, *31*: 645-658. DOI: 10.1071/FP04013.

Brodribb, T J and McAdam, S A M (2017). Evolution of the stomatal regulation of plant water content. *Plant Physiol.*, *174*: 639-649. DOI: 10.1104/pp.17.00078.

Brum, M; Oliveira, R S; López, J G; Licata, J; Pypker, T; Chia, GS; Tinôco, R S and Asbjornsen, H (2020). Effects of irrigation on oil palm transpiration during ENSO-induced drought in the Brazilian Eastern Amazon. *Agric. Water Manag.*, *245(4)*: 1-11. DOI: 10.1016/j.agwat.2020.106569.

Burgess, S S O; Adams, M A; Turner, N C; Beverly, C R; Ong, C K; Khan, A A H and Bleby, T M (2001). An improved heat pulse method to measure low and reverse rates of sap flow in woody plants. *Tree Physiol.*, *21*: 589-598.

Cai, G; Ahmed, M A; Dippold, M A and Zarebanadkouki, M (2020). Linear relation between leaf xylem water potential and transpiration in pearl millet during soil drying. *Plant Soil*, *447*: 565-578.

Carr, M K V (2011). The water relations and irrigation requirements of oil palm (*Elaeis guineensis* Jacq.): A review. *Exp. Agric.*, *47(4)*: 629-652. DOI: 10.1017/S0014479711000494.

Charrier, G (2020). Extrapolating physiological response to drought through step-by-step analysis of water potential. *Plant Physiol.*, *184(2)*: 560-561. DOI: 10.1104/pp.20.01110.

Cheah, S S and Teh, C B S (2020). Parameterization of the farquhar-von caemmerer-berry C3 photosynthesis model for oil palm. *Photosynthetica*, *58(3)*: 769-779. DOI: 10.32615/ps.2020.020.

Coolong, T; Snyder, J; Warner, R; Strang, J and Surendran, S (2012). The relationship between soil water potential, environmental factors, and plant moisture status for Poblano Pepper Grown using tensiometer-scheduled irrigation. *Int. J. Vegetable Sci.*, *18(2)*: 137-152. DOI: 10.1080/19315260.2011.591483.

Darlan, N H; Pradiko, I; Winarna and Siregar, H H (2016). Effect of *El Niño* 2015 on oil palm performance in central and southern Sumatera. *Jurnal Tanah Dan Iklim*, *40(2)*: 113-120. DOI: 10.21082/jti.v40n2.2016.113-120.

Darwis, A; Nurrochmat, D R; Massijaya, M Y; Nugroho N; Alamsyah, E M; Bahtiar, E T and Safe'I, R (2013). Vascular bundle distribution effect on density and mechanical properties of oil palm trunk. *Asian J. Plant. Sci.*, *12(5)*: 208-2013. DOI: 10.3923/ajps.2013.208.213.

Dierick, D; Kunert, N; Köhler, M; Schwendenmann, L and Hölscher, D (2010). Comparison of tree water use characteristics in reforestation and agroforestry stands across the tropics. *Tropical Rainforests and Agroforests under Global Change: Ecological and Socio-economic Valuations* (Tscharntke, T; Leuschner, C; Veldkamp, E; Faust, H; Guhardja, E and Bidin, A eds.). Springer, Berlin. p. 293-308.

Dixon, M and Downey, A (2013). *PSY1 Stem Psychometer Manual Ver. 4.7*. ICT International, Armidale. 162 pp.

Doorenbos, J and Pruitt, W O (1977). Guidelines for predicting crop water requirements. *FAO Irrigantion and Drainage Paper*. p. 1-144.

Dufrene, E and Saugier, B (1993). Gas exchange of oil palm in relation to light, vapour pressure deficit, temperature and leaf age. *Funct. Ecol.*, *7(1)*: 97-104. DOI: 10.2307/2389872.

Ellsäßer, F: Röll, A; Ahongshangbam, J; Waite, P A; Hendrayanto; Schuldt, B and Hölscher, D (2020). Predicting tree sap flux and stomatal conductance from drone-recorded surface temperatures in a mixed agroforestry system- A machine learning approach. *Remote Sens.*, *12(24)*: 1-20. DOI: 10.3390/rs12244070.

Engineer, C; Hashimoto-Sugimoto, M; Negi, J; Israelsson-Nordstrom, M; Azoulay-Shemer, T; Rappel, W J; Iba, K and Schroeder, J (2016). CO_2 sensing and CO_2 regulation of stomatal conductance: Advances and open questions. *Trends Plant Sci.*, *21(1)*: 16-30. DOI: 10.1016/j.tplants.2015.08.014.

Ferrara, G and Flore, J A (2003). Comparison between

different methods for measuring transpiration in potted apple trees. *Biol. Plantarium*, *46(1)*: 41-47. DOI: 10.1023/A:1022301931508.

Figueroa, C M and Lunn, J E (2016). Topical review on sugars a tale of two sugars: Trehalose 6-phosphate and sucrose. *Plant Physiol.*, *172:* 7-27. DOI: 10.1104/pp.16.00417.

Francesconi, A; Lakso, A and Denning, S (1997). Light and temperature effects on whole-canopy net carbon dioxide exchange rates of apple trees. *Acta Hortic.*, *451*: 287-294.

Fricke, W (2017). Water transport and energy. *Plant Cell Environ.*, *40(6)*: 977-994. DOI: 10.1111/pce.12848.

Fricke, W (2019). Night-time transpiration – favouring growth? *Trends Plant Sci.*, *24(4)*: 311-317. DOI: 10.1016/j.tplants.2019.01.007.

Garnier, E; Berger, A and Martin, M (1988). How to estimate leaf transpiration from water potential measurements? *Flora*, *181*: 131-135. DOI: 10.1016/S0367-2530(17)30358-4.

Grömping, U (2006). Relative importance for linear regression in R: The package relaimpo. *J Stat. Softw.*, *17(1)*: 1-27. DOI: 10.18637/jss.v017.i01.

Grömping, U (2015). Variable importance in regression models. *WIREs Comput. Stat.*, *7(2)*: 137-152. DOI: 10.1002/wics.1346.

Haijun, L; Cohen, S; Lemcoff, J H; Israeli, Y and Tanny, J (2015). Sap flow, canopy conductance and microclimate in a banana screenhouse. *Agric. For Meteorol.*, *201*: 165-175. DOI: 10.1016/j.agrformet.2014.11.009.

Hardanto, A; Röll, A; Niu, F and Meijide, A (2017). Oil palm and rubber tree water use patterns: Effects of topography and flooding. *Front. Plant Sci.*, *8*: 1-12. DOI: 10.3389/fpls.2017.00452.

Hashim, R; Nadhari, W N A W; Sulaiman, O; Kawamura, F; Hiziroglu, S; Sato, M; Sugimoto, T; Seng, T G and Tanaka, R (2011). Characterization of raw materials and manufactured binderless particleboard from oil palm biomass. *Mater. Des.*, *32*: 246-254. DOI: 10.1016/j.matdes.2010.05.059.

Hernandez, M J; Montes, F; Ruiz, F; Lopez, G and Pita, P (2016). The effect of vapour pressure deficit on stomatal conductance, sap pH and leaf-specific hydraulic conductance in *Eucalyptus globulus* clones grown under two watering regimes. *Ann. Bot.*, *117*: 1063-1071. DOI: 10.1093/aob/mcw031.

Hochberg, U; Rockwell, F E; Holbrook, N M and Cochard, H (2018). Iso/anisohydry: A plant–environment interaction rather than a simple hydraulic trait. *Trends Plant Sci.*, *23(2)*: 112-120. DOI: 10.1016/j.tplants.2017.11.002.

Ismanov, M; Francis, P; Henry, C and Espinoza, L (2019). Relations among sap flow, soil moisture, weather, and soybean plant parameters in high water demand and final growth stages. *Agric. Sci.*, *10*: 371-385. DOI: 10.4236/as.2019.103030.

Kirkham, M B (2014). Sap flow. *Principles of Soil Plant Water Relations*. Academic Press, Oxford. p. 375-390.

Kobayashi, N; Kumagai, T; Miyazawa, Y; Matsumoto, K; Tateishi, M; Lim T K; Mudd, R G; Ziegler, A D; Giambelluca, T W and Yin, S (2014). Transpiration characteristics of a rubber plantation in Central Cambodia. *Tree Physiol.*, *34*: 285-301. DOI: 10.1093/treephys/tpu009.

Kohler, M; Hanf, A; Barus, H; Hendrayanto and Holscher, D (2014). Cacao trees under different shade tree shelter: Effects on water use. *Agroforest Syst.*, *88*: 63-73. DOI: 10.1007/s10457-013-9656-3.

Legros, S; Mialet-Serra, I; Caliman, J-P; Siregar, F A; Clément-Vidal, A and Dingkuhn, M (2009). Phenology and growth adjustments of oil palm (*Elaeis guineensis*) to photoperiod and climate variability. *Ann. Bot.*, *104(6)*: 1171-1182. DOI: 10.1093/aob/mcp214.

Li, J; Zhang, G Z; Xia, L; Wang, Y; Wang, F Z and Li, X M (2019a). Seasonal change in response of stomatal conductance to vapor pressure deficit and three phytohormones in three tree species. *Plant Signal. Behav.*, *14(12)*: 1-11. DOI: 10.1080/15592324.2019.1682341.

Li, J; Mamtimin, A; Zhaogou, L; Jiang, C and Minzhong, W (2019b). Effects of summer rainfall on the soil thermal properties and surface energy balances in the badain jaran desert. *Adv. Meteorol.*, *2019*: 1-13. DOI: 10.1155/2019/4960624.

Lide, D R (1992). *CRC Handbook of Chemistry and Physics: A Ready Reference Book of Chemical and Phyical Data*. CRC Press, Boca Raton. 658 pp.

Lindeman, R H; Merenda, P F and Gold, R Z (1980). *Introduction to Bivariate and Multivariate Analysis.* Scott, Foresman and Company, Glenview. 444 pp.

Madurapperuma, W S; Bleby, T M and Burgess, S S O (2009). Evaluation of sap flow methods to determine water use by cultivated palms. *Environ. Exp. Bot.*, *66*: 372-380. DOI: 10.1016/j.envexpbot.2009.04.002.

Martínez-Vilalta, J and Garcia-Forner, N (2017).

Water potential regulation, stomatal behaviour and hydraulic transport under drought: deconstructing the iso/anisohydric concept. *Plant Cell Environ.*, *40(6)*: 962-976). DOI: 10.1111/pce.12846.

Massonnet, C; Costes, E; Rambal, S; Dreyer, E and Regnard, J L (2007). Stomatal regulation of photosynthesis in apple leaves: Evidence for different water-use strategies between two cultivars. *Ann. Bot.*, *100*: 1347-1356. DOI: 10.1093/aob/mcm222.

Matheny, A M; Bohrer, G; Vogel, C S; Morin, T H; He, L; Prata De Moraes Frasson, R; Mirfenderesgi, G; Schäfer, K V R; Gough, C M; Ivanov, V Y and Curtis, P S (2014). Species-specific transpiration responses to intermediate disturbance in a northern hardwood forest. *J. Geophys. Res.: Biogeosci.*, *119*: 2292-2311. DOI: 10.1002/2014JG002804.

McJannet, D; Fitch, P; Disher, M and Wallace, J (2007). Measurements of transpiration in four tropical rainforest types of North Queensland, Australia. *Hydrol. Process*, *21*: 3549-3564. DOI: 10.1002/hyp.6576.

Meijide, A; Röll, A; Fan, Y; Herbst, M; Niu, F; Tiedemann, F; June, T; Rauf, A; Hölscher, D and Knohl, A (2017). Controls of water and energy fluxes in oil palm plantations: Environmental variables and oil palm age. *Agric. For Meteorol.*, *239*: 71-85. DOI: 10.1016/j.agrformet.2017.02.034.

Merten, J; Röll, A; Guillaume, T; Meijide, A; Tarigan, S; Agusta, H; Dislich, C; Dittrich, C; Faust, H; Gunawan, D; Hein, J; Hendrayanto, A; Knohl, A; Kuzyakov, Y; Wiegand, K and Hölscher, D (2016). Water scarcity and oil palm expansion: Social views and environmental processes. *Ecol. Soc.*, *21(2)*: 5. DOI: 10.5751/ES-08214-210205.

Milne, R; Deans, J D; Ford, E D; Jarvis, P G; Leverenz, J and Whitehead, D (1985). A comparison of two methods of estimating transpiration rates from a sitka spruce plantation. *Boundary-Layer Meteorol.*, *32(1)*: 155-175.

Murray, F (1967). On the computation of saturation vapor pressure. *J. Appl. Meteorol.*, *6*: 203-204.

Nascimento, P T; Castro, G F de and Júnior, J C F B (2018). Water requirement of irrigated and rainfed crops. *Int. J. Hydrol.*, *2(3)*: 338-341. DOI: 10.15406/ijh.2018.02.00093.

Niu, F; Röll, A; Hardanto, A; Meijide, A; Köhler, M and Hölscher, D (2015). Oil palm water use: Calibration of a sap flux method and a field measurement scheme. *Tree Physiol.*, *35*: 563-573. DOI: 10.1093/treephys/tpv013.

Obilor, E I and Amadi, E C (2018). Test for significance of Pearson's Correlation Coefficient (r). *Int. J. Innov. Math. Stat. Energy Policies*, *6(1)*: 11-23.

Ocheltree, T W; Nippert, J B and Prasad, P V V (2014). Stomatal responses to changes in vapor pressure deficit reflect tissue-specific differences in hydraulic conductance. *Plant Cell Environ.*, *37:* 132-139. DOI: 10.1111/pce.12137.

Otieno, D; Li, Y; Liu, X; Zhou, G; Cheng, J; Ou, Y; Liu, S; Chen, X; Zhang, Q; Tang, X; Zhang, D; Jung, E Y and Tenhunen, J (2017). Spatial heterogeneity in stand characteristics alters water use patterns of mountain forests. *Agric. For. Meteorol.*, *236*: 78-86. DOI: 10.1016/j.agrformet.2017.01.007.

Pereira, L S and Alves, I (2005). Crop water requirements. *Encyclopedia of Soils in the Environment*. Elsevier, New York. p. 322-334.

Phillips, N G; Lewis, J D; Logan, B A and Tissue, D T (2010). Inter-and intra-specific variation in nocturnal water transport in Eucalyptus. *Tree Physiol.*, *30*: 586-596. DOI: 10.1093/treephys/tpq009.

Pradiko, I; Farrasati, R; Rahutomo, S; Ginting, E N; Candra, D A A; Krissetya, Y A and Mahendra, Y S (2020). Pengaruh iklim terhadap dinamika kelembaban tanah di piringan pohon tanaman kelapa sawit. *Warta PPKS*, *25(1)*: 39-51.

Pradiko, I; Ginting, E N; Darlan, N H; Winarna and Siregar, H H (2016a). *Hubungan pola curah hujan dan performa tanaman kelapa sawit di Pulau Sumatra dan Kalimantan selama* El Nino *2015. Jurnal Penelitian Kelapa Sawit, 24(2)*: 87-96. DOI: 10.22302/iopri.jur.jpks.v24i2.11.

Pradiko, I; Hidayat, F; Darlan, N H; Santoso, H; Rahutomo, S and Sutarta, E S (2016b). Ukuran lubang tanam dan aplikasi tandan kosong sawit yang berbeda. *Jurnal Penelitian Kelapa Sawit*, *24(1)*: 23-36. DOI: 10.22302/iopri.jur.jpks.v24i1.4.

Rivera-Méndez, Y D; Chacón, L M; Bayona, C J and Romero, H M (2012). Physiological response of oil palm interspecific hybrids (*Elaeis oleifera* H.B.K. Cortes versus *Elaeis guineensis* Jacq.) to water deficit. *Braz. J. Plant Physiol.*, *24(4)*: 273-280. DOI: 10.1590/S1677-04202012000400006.

Roddy, A B; Winter, K and Dawson, T E (2013). Sap flow through petioles and petiolules reveals leaf-level responses to light and vapor pressure deficit in the tropical tree *Tabebuia rosea* (*Bignoniaceae*).

bioRxiv. p. 30-34. DOI: 10.1101/000711.

Röll, A; Niu, F; Meijide, A; Hardanto, A; Hendrayanto; Knohl, A and Hölscher, D (2015). Transpiration in an oil palm landscape: Effects of palm age. *Biogeosciences*, *12(19)*: 5619-5633. DOI: 10.5194/bg-12-5619-2015.

Ruiz-Penalver, L; Vera-repullo, J A; Jiménez-buendía, M; Guzman, I and Molina-Martinez, J M (2015). Development of an innovative low cost weighing lysimeter for potted. *Agric. Water Manag*., *151*: 103-113. DOI: 10.1016/j.agwat.2014.09.020.

Santi, L P; Ardiyanto, A; Kurniawan, A; Prabowo, L A and Sebastian, I (2021). Improvement of water and nutrient efficiencies oil palm through bio-silicic acid application. *Menara Perkebunan*, *89(1)*: 26-36. DOI: 10.22302/iribb.jur.mp.v89i1.409.

Satriawan, H; Fuady, Z and Fitri, R (2021). Soil erosion control in immature oil palm plantation. *J. Water Land Dev.*, *49*: 47-54. DOI: 10.24425/jwld.2021.137095.

Sitková, Z; Nalevanková, P; Střelcová, K; Fleischer, P; Ježík, M; Sitko, R; Pavlenda, P and Hlásny, T (2014). How does soil water potential limit the seasonal dynamics of sap flow and circumference changes in European beech? *Forestry Journal*, *60(1)*: 19-31. DOI: 10.2478/forj-2014-0002.

Smith, D M and Allen, S J (1996). Measurement of sap flow in plant stems. *J. Exp. Bot.*, *47(305)*: 1833-1844. DOI: 10.1093/jxb/47.12.1833.

Steppe, K; Vandegehuchte, M W; Tognetti, R and Mencuccini, M (2015). Sap flow as a key trait in the understanding of plant hydraulic functioning. *Tree Physiol.*, *35(4)*: 341-345. DOI: 10.1093/treephys/tpv033.

Su, Y; Shao, W; Vlcek, L and Langhammer, J (2019). Ecohydrological behaviour of Mountain Beech Forest: Quantification of stomatal conductance using sap flow measurements. *Geoscience*, *9(243)*: 1-16. DOI: 10.3390/geosciences9050243.

Suresh, K; Nagamani, C; Kantha, D L and Kumar, M K (2012a). Changes in photosynthetic activity in five common hybrids of oil palm (*Elaeis guineensis* Jacq.) seedlings under water deficit. *Photosynthetica*, *50(4)*: 549-556. DOI: 10.1007/s11099-012-0062-2.

Suresh, K; Kiran, K M; Lakshmi, K D; Prasanna, L R and Sunil, K K (2012b). Variations in photosynthetic parameters and leaf water potential in oil palm grown under two different moisture regimes. *Indian J. Plant Physiol.*, *17(3-4)*: 233-240.

Tran, N; Bam, P; Black, K; Graham, T; Zhang, P; Dixon, M; Reeves, B and Downey, A (2015). Improving irrigation scheduling protocols for nursery trees by relating cumulative water potential to concurrent vapour pressure. *Acta Hortic.*, *1085*: 129-134. DOI: 10.17660/ActaHortic.2015.1085.22.

Villalobos-González, L; Muñoz-Araya, M; Franck, N and Pastenes, C (2019). Controversies in midday water potential regulation and stomatal behavior might result from the environment, genotype, and/or rootstock: Evidence from Carménère and Syrah grapevine varieties. *Front. Plant Sci.*, *10*: 1-15. DOI: 10.3389/fpls.2019.01522.

Waite, P; Schuldt, B; Link, R M; Breidenbach, N; Triadiati, T; Hennings, N; Saad, A and Leuschner, C (2019). Soil moisture regime and palm height influence embolism resistance in oil palm. *Tree Physiol.*, *39(10)*: 1696-1712. DOI: 10.1093/treephys/tpz061.

Wang, X; Zhang, W and Liu, X (2013). Daily variations in transpiration rate and water potential of *Robinia pseudoacacia*. *J. Food Agric. Environ.*, *11(1)*: 999-1005.

Xu, S and Yu, Z (2020). Environmental control on transpiration: A case study of a desert ecosystem in Northwest China. *Water*, *12:* 1-16. DOI: 10.3390/W12041211.

Yono, D; Purwanti, E; Sahara, A; Nugroho, Y A; Tanjung, Z A; Aditama, R; Dewi, C; Sihotang, A E; Utomo, C and Liwang, T (2019). Physiology and genotyping of adaptive and sensitive oil palm progenies under unwatered stress condition physiology and genotyping of adaptive and sensitive oil palm progenies under unwatered stress condition. *Proc. of the 2nd International Conference on Natural Resources and Life Sciences*. *IOP Conf. Ser.: Earth Environ. Sci.* Surabaya, Indonesia. p. 1-11.

Zha, T; Qian, D; Jia, X; Bai, Y; Tian, Y; Bourque, C P A; Ma, J; Feng, W; Wu, B and Peltola, H (2017). Soil moisture control of sap-flow response to biophysical factors in a desert-shrub species, *Artemisia ordosica*. *Biogeosciences*, *14(19):* 4533-4544. DOI: 10.5194/bg-14-4533-2017.

Zhang, H; Morison, J I L and Simmonds, L P (1999). Transpiration and water relations of poplar trees growing close to the water table. *Tree Physiol.*, *19(9)*:

563-573. DOI: 10.1093/treephys/19.9.563.

Zhang, D; Du, Q; Zhang, Z; Ji, X; Song, X and Li, J (2017). Vapour pressure deficit control in relation to water transport and water productivity in greenhouse tomato production during summer. *Sci. Rep*., *4:* 1-11. DOI: 10.1038/srep43461.

Zhang, Q; Manzoni, S; Katul, G; Porporato, A and Yang, D (2014). The hysteretic evapotranspiration-vapor pressure deficit relation. *J. Geophys. Res. Biogeosci*., *119:* 125-140. DOI: 10.1002/2013JG002484.

Zhang, Q; Jia, X; Shao, M; Zhang, C; Li, X and Ma, C (2018). Sap flow of black locust in response to short-term drought in southern Loess Plateau of China. *Sci Rep*., *8:* 1-10. DOI: 10.1038/s41598-018-24669-5.

Zhao, W; Liu, B; Chang, X; Yang, Q; Yang, Y; Liu, Z; Cleverly, J and Eamus, D (2016). Evapotranspiration partitioning, stomatal conductance, and components of the water balance: A special case of a desert ecosystem in China. *J. Hydrol*., *538*: 374-386. DOI: 10.1016/j.jhydrol.2016.04.042.